Green Chemistry

Synthesis of performance-advantaged polyurethanes and polyesters from biomass-derived monomers by aldol-condensation of 5-hydroxymethyl furfural and hydrogenation

Journal:	*Green Chemistry*
Manuscript ID	GC-ART-03-2021-000899.R1
Article Type:	Paper
Date Submitted by the Author:	08-Apr-2021
Complete List of Authors:	Chang, Hochan; University of Wisconsin Madison, Chemical and Biological Engineering Gilcher, Elise; University of Wisconsin, Chemical and Biological Engineering Huber, George; University of Wisconsin, Chemical and Biological Engineering Dumesic, James; University of Wisconsin Madison, Chemical and Biological Engineering

ARTICLE

Synthesis of performance-advantaged polyurethanes and polyesters from biomass-derived monomers by aldol-condensation of 5-hydroxymethyl furfural and hydrogenation

Received 00th January 20xx,
Accepted 00th January 20xx

DOI: 10.1039/x0xx00000x

Hochan Chang[a], Elise B. Gilcher[a,b], George W. Huber[a], and James A. Dumesic[a,b*]

Functional polyurethanes and polyesters with tunable properties were synthesized from biomass-derived 5-hydroxymethyl furfural (HMF)-Acetone-HMF (HAH) monomers. HAH can be selectively hydrogenated over Cu and Ru catalysts to produce partially-hydrogenated (PHAH) and fully-hydrogenated (FHAH). The HAH units in these polymers improve the thermal stability and stiffness of the polymers compared to polyurethanes produced with ethylene glycol. Polyurethanes produced from PHAH provide diene binding sites for electron deficient C=C double bonds, such as in maleimide compounds, that can participate in Diels-Alder reactions. Such sites can function to create crosslinking by Diels-Alder coupling with bismaleimides and can be used to impart functionality to PHAH (giving rise to anti-microbial activity or controlled drug delivery). The symmetric triol structure of FHAH leads to energy-dissipating rubbers with branched structures. Accordingly, the properties of these biomass-derived polymers can be tuned by controlling the blending ratio of HAH-derived monomers or the degree of Diels-Alder reaction. The polyester produced from HAH can be used in packaging applications.

Introduction

The use of renewable biomass resources for the production of fuels, chemicals, and materials for society has been a direction of recent research and development[1,2]. One of the key problems encountered in the implementation of new processes for the production of products from renewable biomass resources[1,3,4] is that these processes must economically compete with currently established, processes for the production of products from non-renewable petroleum resources[5–7]. The economic justification required to fund new pioneer processes is oftentimes hard to accomplish unless the products produced biomass have properties that are superior compared to the corresponding products currently produced from petroleum. One main advantage of biomass-feedstocks is that they have higher oxygen functionality than petroleum-derived molecules making them candidates to create new performance-advantaged polymers. In the present paper, we show that it is possible to produce a suite of new performance advantaged polyurethanes and polyesters from biomass-derived C_6-sugar monomers. The cost for production of these new monomers[4] is competitive with the cost for production of petroleum-derived monomers[8].

Polyurethanes are used in a wide range of applications including insulators, foams, paints, coatings, elastomers, inks, and integral skins[9]. The urethane bonds in polyurethanes are synthesized by the reaction of diols with diisocyanates. The most common diols are ethylene glycol, 1,4-butanediol, and 1,6 hexanediol. The thermal and physical properties of polyurethanes can be modified by the use of different types of diisocyanates[10]. The molar ratio of the monomers influence the polymer properties[11] and the degree of crosslinking[12]. Generally, flexible long segments of polyols produce soft viscoelastic polymers, whereas stiff polymers are synthesized by a higher degree of crosslinking. Thus, stretchy polymers are obtained through long chains with low crosslinking, while hard polymers are yielded from shorter chains with high crosslinking. A combination of long chains with average degree of crosslinking produces foam shapes of polymers[9]. Polyesters are also used in a wide range of applications including packaging, adhesives[13], and biomedical applications[14]. Polyesters are produced by ring-opening reactions[15] or esterification of a diol with a dicarboxylic acid. Similarly, the properties of the polyester can be tuned by changing the type and ratio of dicarboxylic acid and the diols used[16].

The industrial polyols used today are almost exclusively derived from petroleum. Environmental concerns have led research towards sustainable and eco-friendly substitutes from natural resources[17]. Several studies have produced polymers from biomass-derived feedstocks. Polyols, derived from vegetable oils, were used to produce polyurethanes[18]. However, production of polyols from vegetable oils is expensive, requiring multiple reaction steps, including epoxidation, hydroformylation, ozonolysis, transetherification, amination, and tiol-ene couplings[18]. 5-

[a] Department of Chemical and Biological Engineering, University of Wisconsin–Madison, Madison, WI, USA.
[b] DOE Great Lakes Bioenergy Research Center, University of Wisconsin–Madison, Madison, WI, USA.
*Corresponding author. E-mail: jdumesic@wisc.edu
† Footnotes relating to the title and/or authors should appear here.
Electronic Supplementary Information (ESI) available: [details of any supplementary information available should be included here]. See DOI: 10.1039/x0xx00000x

hydroxymethyl furfural (HMF) is a biomass-derived platform chemical that can be effectively synthesized from corn starch[1]. HMF can be used to produce furan dicarboxylic acid (FDCA) which is then reacted with ethylene glycol to create polyethylene 2,5-furandicarboxylate (PEF). This technology is being commercialized by Avantium and AVA Biochem[19] as a polyester with improved barrier properties[20]. A HMF-derived diol was synthesized by acetalization with pentaerythriol and used as a diol resource for production of poly(urethane-urea)s and polyesters[21]. Unfortunately, HMF-derived diols can be chemically unstable due to the furanic functionality which leads to uncontrollable ring-opening and/or condensation reactions[22] when the composition of biomass-derived monomers is high in the feed. Kraft lignin has also been used to synthesize polyurethanes[23] or to blend with polyesters[24]. However, the lignin and polyurethane network becomes brittle when the lignin content is above 30-35%[23]. Therefore, the use of chemically stable petroleum-based aliphatic diols, such as ethylene glycol, 1,4-butanediol, and 1,6-hexandiol, is necessary to utilize the biomass-derived polyols in polymer synthesis. Accordingly, the composition of biomass-based polyols in polymers has been limited to achieve advantaged polymeric properties. Past research in using biomass-derived monomers for polymer synthesis has identified several challenges including: 1) the high cost to produce biomass-based monomers, 2) the use of additional petrochemicals for polymer synthesis and 3) the lack of the polymer fitting into the current infrastructure.

We have previously shown that HMF and acetone can be converted into the HMF-Acetone-HMF (HAH) diol by base-catalyzed aldol condensation[25]. HAH contains functional groups, including hydroxyl, furan, enone, and ketone functionalities, that can be exploited to further tune the polymer properties[25]. The π-electron conjugation between the enone and furan groups in HAH monomer stabilizes the furan group to prevent the uncontrolled degradation of furans during reactions, such as etherification at 180℃[4]. Techno-economic analysis for HAH production from fructose indicates that HAH can be produced at similar costs (1000-2500 $ ton^{-1})[4] as petroleum-derived diols, such as ethylene glycol (1000-1400 $ ton^{-1})[8]. Moreover, fructose and glucose can be effectively synthesized from non-edible biomass, such as corn stover, hardwood and softwood,[26] for use as feedstocks for HAH[4] and HMF production[1]. Therefore, HAH is a renewable monomer that can be used to synthesize polymers, having high molecular weight (274 g mol^{-1}), symmetric functionalities, an inexpensive production price, and being derived from renewable resources without competition with food resources. Here, we demonstrate the synthesis of functional polyurethanes and a renewable polyester (Figure 1) from HAH-derived monomers, 4,4'-methylenebis(phenyl isocyanate) (MDI), and succinic acid (SA). These biomass-derived polymers have additional chemical functionality that can be used to give the polymer additional properties.

Results and Discussion

Synthesis of biomass-derived monomers

Cu and Ru catalyst showed different hydrogenation reactivities toward the furan rings. The furan rings in the HAH molecules were intact when Cu was used for hydrogenation, whereas Ru can effectively hydrogenate all double bonds in the enone and furan groups. As a result, Cu/γ-Al_2O_3 catalyst selectively hydrogenated the carbon double bonds (C=C) in the enone groups of HAH to produce partially-hydrogenated HAH (PHAH) in IPA solvent at 120℃. It is possible that the high selectivity for production of PHAH over Cu compared to Ru is caused by weaker binding of reaction intermediates over Cu, combined with the higher thermodynamic driving force for hydrogenation of C=C bonds in alkenes compared to hydrogenation of C=C bonds in furans and C=O bonds[27,28]. After 12 h of hydrogenation at 120℃, 100 mol% of HAH was converted to PHAH in 91 mol% yield. A dehydrated by-product of this reaction was also detected (Figure S1). At temperatures higher than 120℃, production of the by-products became significant. Ru/C catalyst hydrogenated HAH to fully-hydrogenated HAH (FHAH) at 180℃ after 1 h of reaction in 100 mol% yield without significant side reactions (Figure S2). The reaction pathway of metal-catalyzed HAH hydrogenation and polymerization of HAH-derived monomers are shown in Scheme1.

ARTICLE

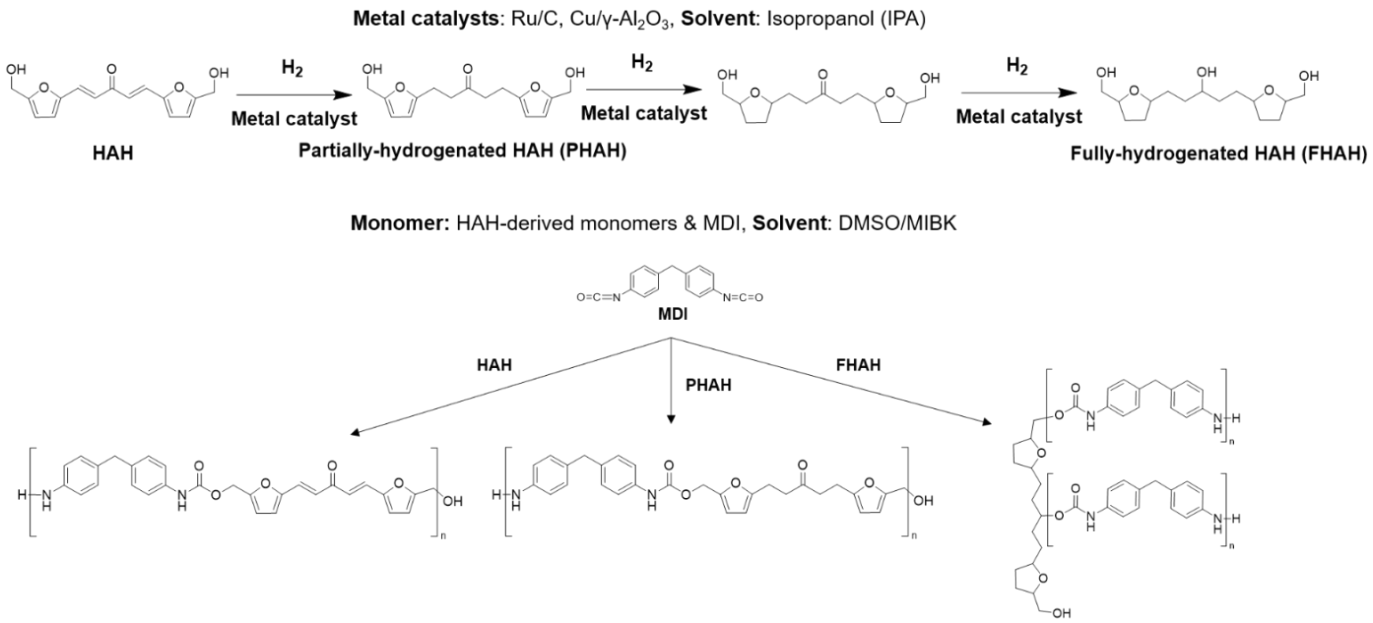

Scheme 1. Metal catalyzed hydrogenation of HAH to produce partially-hydrogenated HAH (PHAH) and fully-hydrogenated HAH (FHAH) for production of HAH-derived monomers and the polymerization of HAH-derived monomers with MDI for production of HAH-derived polymers.

Synthesis and characterization of biomass-derived polyurethanes

A wide variety of polyurethanes and one polyester were synthesized from HAH, FHAH and PHAH as shown in Figure 1. HAH solution in DMSO solvent and MDI solution in MIBK (HAH/MDI (mol) = 1.0 in feed) were reacted to synthesize the HAH-MDI polyurethane (Figure S3, Figure 1.A) without a catalyst. The storage modulus of HAH-MDI was measured to be 1.6-4.0 MPa, and the ratio of loss modulus to storage modulus (tanδ) was 0.17-0.19 by DMA analysis (Figure S14.A). These modulus values indicate that HAH-MDI is a stiff elastic rubber. FHAH-MDI (Figure S5, Figure 1.C) was synthesized (FHAH/MDI (mol) = 1.0 in feed), and the storage modulus of FHAH-MDI was measured to be 0.3-2.1 MPa. The value of tanδ of FHAH-MDI ranged between 0.2 and 1.1 (Figure S14.B) indicating that FHAH-MDI is a viscous (energy-dissipating) polyurethane (Figure S5). The difference in the stiffness of the polyurethanes results from the molecular orbitals of the biomass-derived monomers that comprise the backbone of the polyurethanes. HAH consisted of sp^2 carbons, which provide a rigid frame of the monomer, whereas FHAH contained sp^3 carbons and has high flexibility. Consequently, HAH-based polyurethane is a stiff rubber, but the highly flexible structure of FHAH provides a soft energy-dissipating rubber. The polyurethanes can be shaped by curing the monomer solution in molds (Figure 1.J and K) or used to provide hydrophobic coating (Figure S13.B and D) on glass by covering the glass with a thin layer of the monomer solution, followed by curing. The color of HAH-MDI coating was yellow (Figure S13.A) The color difference between the molded (Figure 1.J and K) and the coated samples (Figure S13.A and B) resulted from the thickness of the samples. Accordingly, the thicker molded samples (mm scale) display darker color than thinner coated samples (μm scale). HAH-MDI could thus be used as a coating for UV-blocking because chromophores in the HAH units that absorb UV light with large (22,262 $M^{-1}cm^{-1}$ at 378 nm) molar excitation coefficient[4] remained intact in the polymer structure. The energy-dissipating property of FHAH-MDI (Figure S13.C) could be used as an impact-resistant coating or in packaging applications. HAH-MDI is a linear polyurethane that consists of equivalent diol and diisocyanate units in the polymeric structure (by ^{13}C qNMR). However, FHAH-MDI is a branched polyurethane with a 1 to 2 molar ratio of FHAH and MDI (by ^{13}C qNMR). Equimolar ratio of isocyanate to hydroxyl groups in the feed resulted in hydroxymethyl ($-CH_2OH$) and amine ($-NH_2$) terminal groups in HAH-MDI, PHAH-MDI, and FHAH-MDI. The terminal groups and degree of polymerization (DP) were characterized by ^1H NMR in Figure S3-5 and S19. Amine terminal groups were produced from the reaction of isocyanate terminal groups and water when the polyurethanes were washed by water to remove DMSO and MIBK solvents. ATR-FTIR analysis also indicated the presence of amine and hydroxyl terminal groups, formation of urethane bonds, and disappearance of isocyanate groups (~2270 cm^{-1})[29] in the molded polyurethanes (Figure S20).

The molar ratio of the stable urethane (NHCOO) group to the hydroxymethyl (CH_2OH) group was used to calculate the DP by ^1H NMR in Figure S3-5 and S19. We note that the DP of each polyurethane depends on the reactivity of the monomer and the reaction time. For example, the least stable monomer, PHAH, has DP=9~10 (Figure S4 and S17.B) after 5 min of polymerization, while more stable monomers, such as HAH and FHAH, only achieve DP=4~5 (Figure S3, S5, S17.A and C) after 5 min of reaction. The DP of HAH-MDI and FHAH-MDI increased from 4-5 to 10 (Figure S19) by curing the mixed monomer solution for a longer time (23 h) in a mold at 50℃ (Figure 1.J and K).

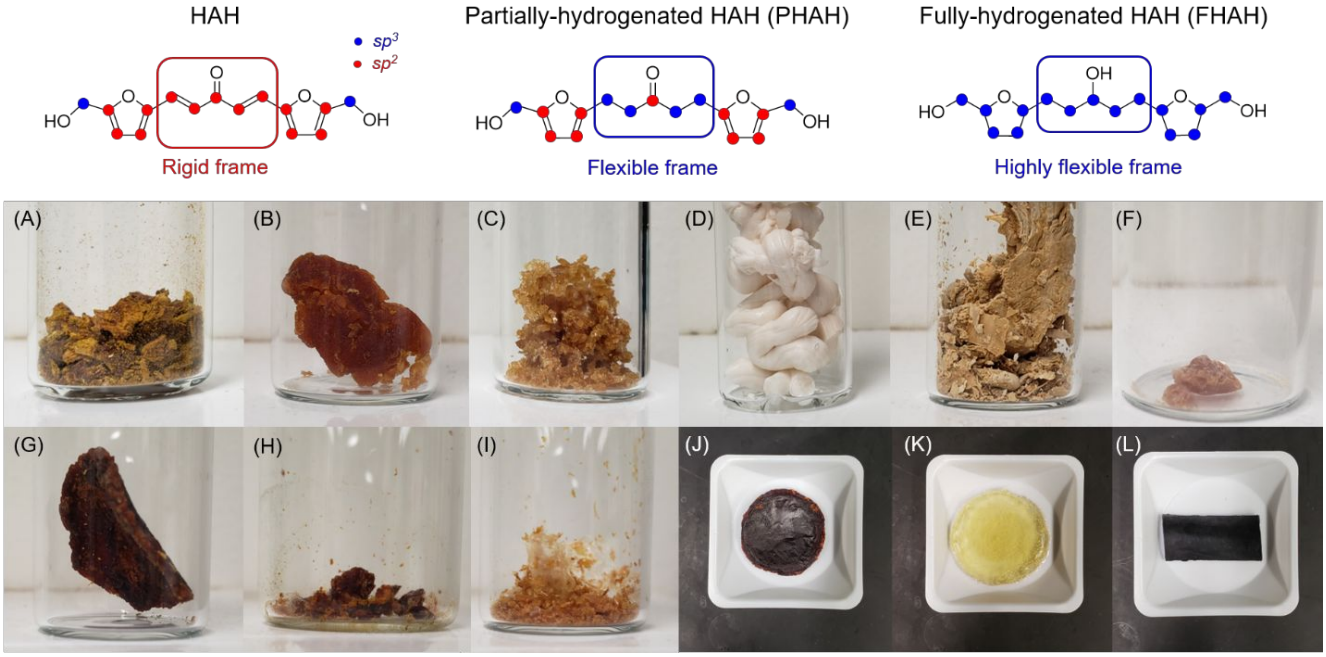

Figure 1. Molecular structure of biomass-derived monomers and pictures of the polyurethanes and a polyester (A) HAH-MDI, (B) PHAH-MDI, (C) FHAH-MDI, (D) EG-MDI, (E) 70% EG-30% PHAH-MDI, (F) PHAH-MDI after 26% Diels-Alder crosslinking, (G) 23% HAH-77% PHAH-MDI, (H) 23% HAH-77% PHAH-MDI after 39% Diels-Alder crosslinking, (I) 70% EG-30% PHAH-MDI after 15% Diels-Alder crosslinking, (J) circular molded HAH-MDI, (K) circular molded FHAH-MDI, and (L) rectangular molded HAH-SA polyester (% represents mol% and EG indicates ethylene glycol).

Synthesis of polyurethanes from blended diols and MDI

The biomass-derived monomers can be blended with each other or with petroleum-based monomers, such as ethylene glycol (EG), to produce polyurethanes. 2.33 equivalent EG and PHAH were used as a diol feed for synthesizing a blended polyurethane with MDI (70% EG-30% PHAH-MDI, Figure 1.E). This blended polyurethane was characterized by HSQC and ^{13}C qNMR (Figure S8). PHAH can be blended with HAH and produced a blended polyurethane (23% HAH-77% PHAH-MDI, Figure 1.G). The blended polyurethane was characterized by HSQC and ^{13}C qNMR (Figure S9). The PHAH units in the blended polyurethanes can be used to provide maleimide-appending sites by Diels-Alder reaction.

Diels-Alder reactions of polyurethanes comprising PHAH

The diene functionality in the furan ring of HAH has no reactivity for Diels-Alder reaction with maleimide because of a nearby electron-withdrawing C=C bond. Catalytic conversions of electron-withdrawing groups to electron-donating groups activated the diene functionality in the furan ring and enabled Diels-Alder reaction.[30] Thus, maleimide was coupled with the furan ring of PHAH in THF solvent at 50℃ after hydrogenation converted the electron-withdrawing C=C bonds to electron-donating C-C bonds. After 93 h of Diels-Alder reaction, 83 mol% of the furan moiety (Maleimide/furan in feed (mol) = 1.48) in PHAH was coupled with maleimide, as shown in Figure 2.A. The molecular structure of Diels-Alder coupled PHAH and maleimide were characterized by HSQC and ^{13}C qNMR (Figure S6).

PHAH was reacted with an equivalent amount of MDI to synthesize PHAH-MDI polyurethane (Figure S4, Figure 1.B). Diels-Alder reaction of PHAH-derived polyurethanes with bismaleimide was then investigated. Bismaleimide was dissolved in THF solvent and reacted with the THF-swollen PHAH-MDI. The bismaleimide provided 26 mol% of crosslinking by Diels-Alder reaction (PHAH unit/Bismaleimide (mol) = 3.34 in feed, 86 mol% conversion of bismaleimide after 69 h, Figure 1.F). The blended polyurethane with 23 mol% of HAH and 77 mol% of PHAH as diol units (HAH-PHAH-MDI) was reacted with bismaleimide and provided 39 mol% of Diels-Alder crosslinking (PHAH unit/Bismaleimide (mol) = 2.00 in feed, 78 mol% conversion of bismaleimide after 70 h, Figure 1.H). Another blended polyurethane that was comprised of 70 mol% EG and 30 mol% PHAH as diol units (EG-PHAH-MDI) showed 48 mol% conversion of bismaleimide after 70 h of reaction (PHAH unit/Bismaleimide (mol) = 1.00 in feed, 15 mol% of Diels-Alder crosslinking, Figure 1.I). The conversion of bismaleimide remained constant (48 mol%) after 165 h of reaction. Thus, the conversion of bismaleimide by Diels-Alder reaction decreased as the molar composition of PHAH units in polyurethanes decreased (Figure 2.B). Bismaleimide and the crosslinked polyurethane showed significant difference in solubility toward THF and DMSO solvents. For example, bismaleimide has high solubility in THF (>40 mg/mL at

25°C) and DMSO (>200 mg/mL at 25°C), whereas the polyurethane has limited solubility in THF (<3 mg/mL at 25°C) and DMSO (<3 mg/mL at 25°C), as shown in Figure S18. The significant solubility difference of bismaleimide and the crosslinked polyurethanes enabled simple separation of the unreacted bismaleimide from the polyurethanes. The unreacted bismaleimide was completely solubilized in THF and removed by separation of THF solution from the precipitated polyurethanes after Diels-Alder reaction. The structures of the crosslinked PHAH-MDI and EG-PHAH-MDI were analyzed by NMR analyses and included chemical shifts from Diels-Alder adducts and unwashed bismaleimide (Figure S7 and S10). The higher degree of Diels-Alder crosslinking reduced the solubility of the polyurethanes; therefore, the structure of HAH-PHAH-MDI could not be characterized by NMR because the polymer was not soluble in DMSO-d_6 solvent after 39% of Diels-Alder crosslinking.

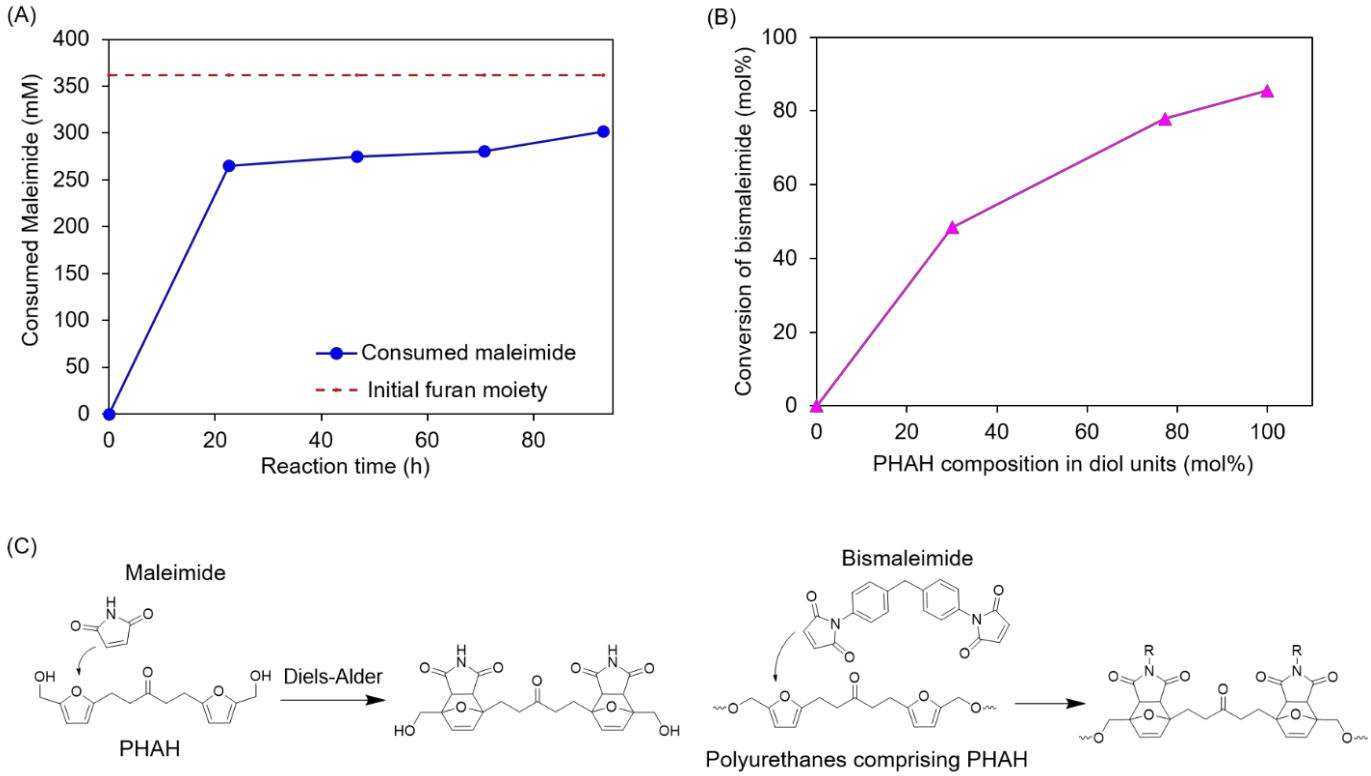

Figure 2. (A) Concentration of the consumed maleimide by Diels-Alder rection with furan moiety in PHAH as a function of reaction time (measured by HPLC), (B) Conversion of bismaleimide as a function of PHAH composition in diol units; (C) Schematic Diels-Alder reaction pathway for PHAH and polyurethanes comprising PHAH.

Thermal properties of biomass-derived polymers

The thermal properties of the polymers, having molecular weights of a few thousand g mol^{-1}, were measured by DSC (Figure S15-16) and TGA (Figure S12.A), and the weight-averaged molecular weights ($\overline{MW}$) of THF-soluble oligomers were measured by GPC (Figure S17). These properties are summarized in Table 1. Exothermic transitions include evaporation of solvents and moisture or melting of the polyurethanes. Endothermic transitions involve the formation of crosslinking or crystallization of polyurethanes. It is interesting to note that linear HAH-MDI had a crystalline point at 237°C and became a thermoset plastic polymer after heating at >237°C, whereas the branched FHAH-MDI did not have a crystalline point. We hypothesize that π-electron conjugation in HAH monomer provides physical and/or chemical crosslinking sites to form a crystalline phase by thermal degradation above 237°C. The temperatures, corresponding to 20 wt% and 50 wt% of thermal degradation of the polyurethanes, were represented as $T_{xx\%}$ in Table 1 and are used to compare the thermal stability of polyurethanes. For example, $T_{50\%}$ of HAH-MDI, PHAH-MDI, and FHAH-MDI were measured to be 490, 320, and 360°C, respectively in Table 1. $T_{20\%}$ and $T_{50\%}$ values of HAH-derived polyurethanes indicate that HAH monomer can be used to synthesize thermally stable polyurethanes while PHAH monomer provides the least thermally stable polyurethanes. We note that the furan functional groups remained as intact in polyurethanes by NMR analysis (Figure S3-11) without thermal degradation during polymerization. When HAH replaced EG in the polyurethane the $T_{20\%}$ and $T_{50\%}$ increased from 125 to 240°C and from 310 to 490°C, respectively. HAH-MDI had no glass transition temperature after an exothermic transition at 237°C, while the glass transition temperature of EG-MDI (Figure 1.D) was 80°C. The addition of 23 mol% HAH into PHAH-MDI (HAH-PHAH-MDI) increased the glass transition temperature, $T_{20\%}$ and $T_{50\%}$ of the polyurethane from 68 to 93°C, from 130 to 175°C, and from 320 to 390°C, respectively. These results demonstrate that different composition of HAH units in polyurethanes can be used to tune the thermal stability of polyurethanes. The glass transition temperature, $T_{20\%}$, and $T_{50\%}$ of PHAH were similar to those of EG-MDI. However, 26 mol% of Diels-Alder crosslinking (PHAH-MDI after Diels Alder) increased the glass transition temperature from 68 to 134°C with higher $T_{20\%}$ (180°C) and $T_{50\%}$ (470°C). The addition of

Diels-Alder crosslinking (39 mol%) to HAH-PHAH-MDI (HAH-PHAH-MDI after Diels-Alder) increased $T_{50\%}$ of the HAH-PHAH-MDI from 390 to 510℃. Moreover, the HAH-PHAH-MDI after Diels-Alder became thermally stable after exothermic transition (200℃) and the glass transition temperature was not observed in 2nd and 3rd cycles of DSC. PHAH was blended with EG-MDI (EG-PHAH-MDI) and increased the glass transition temperature from 80 to 134℃, but $T_{50\%}$ was not significantly improved. The glass transition temperature (from 134 to 179℃) and $T_{50\%}$ (from 330 to 440℃) of EG-PHAH-MDI were further improved after PHAH units formed 15 mol% of Diels-Alder crosslinking. The PHAH can be used to produce functional polyurethanes with tunable thermal stability by controlling the degree of Diels-Alder crosslinking with bismaleimide. Polyurethanes are used as thermal insulation materials[31,32]. A higher specific heat capacity of insulators indicates higher performance of the thermal insulation because materials with high specific heat capacity can absorb more heat energy before they increase temperature. HAH-derived polyurethanes had higher specific heat capacity (0.9-1.5 J $℃^{-1}g^{-1}$) than EG-MDI (0.6-0.9 J $℃^{-1}g^{-1}$). Diels-Alder crosslinking did not affect the specific heat capacity. These results indicate that the thermal properties, such as glass transition temperature and thermal stability, of HAH-derived polyurethanes can be tuned.

Table 1. Thermal properties and the weight-averaged molecular weight ($\overline{MW}$) of biomass-derived polymers ($\overline{MW}$ of THF-solubilized polyurethanes were measured by GPC; Exo and endothermic transitions were measured at 1st heating cycle of DSC; Glass transition temperature and specific heat capacity (C_p) were measured at 2nd heating and cooling cycle of DSC; [a]Diol units consisted of 23mol% of HAH and 77mol% of PHAH; [b]Diol units consisted of 70mol% of EG and 30mol% of PHAH; PD abbreviates polydispersity).

	$\overline{MW}$ (g mol^{-1})	PD	Endothermic transition (℃)	Exothermic transition (℃)	Glass transition (℃)	C_p (J $℃^{-1}g^{-1}$)	$T_{20\%}$ (℃)	$T_{50\%}$ (℃)	Char yield (wt%)
EG-MDI	---	---	238	---	80	0.6-0.9	125	310	10
HAH-MDI	4,513	1.62	175	237	---	0.9-1.5	240	490	38
PHAH-MDI	10,262	2.18	196	---	68	0.9-1.5	130	320	21
FHAH-MDI	3,883	1.99	191	---	87	0.9-1.5	165	360	7
PHAH-MDI after 26 % Diels-Alder crosslinked	---	---	127	200	134	0.9-1.5	180	470	35
HAH-PHAH-MDI[a]	8,312	2.13	180	---	93	0.9-1.5	175	390	30
HAH-PHAH-MDI after 39 % Diels-Alder crosslinked	---	---	126	200	---	0.9-1.5	170	510	40
EG-PHAH-MDI[b]	15,583	3.26	170	220	134	0.9-1.5	210	330	19
EG-PHAH-MDI after 15 % Diels-Alder crosslinked	---	---	104	215	179	0.9-1.5	270	400	21
HAH-SA	1,139	1.24	133	---	73	0.9-1.5	220	480	40

Synthesis and characterization of a biomass-derived polyester

Succinic acid (SA) can be synthesized from biomass feedstocks including glucose[33], furfural[34], and lignin[35]. The esterification of HAH and SA produces a renewable polyester (HAH-SA, Figure 1.L). DMSO solvent dissolved the solid phase monomers and dibutyltin oxide catalyst in a homogeneous solution for solution polymerization. ^{13}C qNMR analysis (Figure S11) was used to track the formation of ester bonds between HAH and SA at 130℃. After 870 min of esterification, 50 mol% of HAH (by ^{13}C qNMR) was converted to the polyester. The thermal stability temperatures of HAH-SA (Figure S12.B) were 220℃ and 480℃ for the $T_{20\%}$ and $T_{50\%}$, respectively. After heating at 800℃, 40 wt% of the polyester was converted to char. The glass transition and endothermic transition temperatures were measured to be 73℃ and 133℃, respectively. The specific heat capacity of the polyester was 0.9-1.5 J $℃^{-1}g^{-1}$. The storage modulus of HAH-SA was measured to be 1.0-2.6 MPa, and tanδ (=E"/E') was 0.15-0.23 by DMA analysis (Figure S14.C). Based on the properties of the HAH-SA polyester, the polyester could be used as a flexible UV-blocking packaging material to replace polyethylene terephthalate (PET).

Experimental method

Materials. The following materials were used in all experiments: 5-(hydroxymethyl) furfural (HMF, AK Scientific, 98%), Acetone (Fisher, HPLC grade), 4,4'-methylenebis(phenyl isocyanate) (MDI, Sigma-Aldrich, 98%), Maleimide (99%, Sigma-Aldrich), Bismaleimide (95%, Sigma-Aldrich), Succinic acid (99%, Sigma-Aldrich), Dibutyltin (IV) oxide (98%, Sigma-Aldrich), Dimethyl sulfoxide (DMSO, Sigma-Aldrich, anhydrous, ≥99.9%), 4-methyl-2-pentanone (MIBK, Sigma-Aldrich, HPLC grade), 2-propanol (IPA, HPLC grade, Sigma-Aldrich),Tetrahydrofuran (THF, Sigma-Aldrich), Gamma alumina (Strem Chemicals), Tetraaminecopper(II) sulfate ($[Cu(NH_3)_4]SO_4{\cdot}_xH_2O$, Strem Chemicals), 0.5 M ammonium hydroxide solution (Sigma-Aldrich), 2 M sulfuric acid (Sigma-Aldrich), 5wt% Ru/C catalyst (Sigma-Aldrich), NaOH (FCC specification, Fisher Scientific), HCl (37 wt%, Sigma-Aldrich), Milli-Q water (~18 MΩ cm). Hydrogenation was performed in a 50 mL Parr reactor (Parr Instrument Company).

HPLC analysis of Diels-Alder reactions. The chemical concentrations of maleimide and bismaleimide were quantified by high performance liquid chromatography (HPLC) analysis. The maleimide containing solutions were diluted by 10 times with Milli-Q water and the bismaleimide containing solutions were diluted by 5 times in acetone. All the diluted solutions were filtered through 0.2 µm PTFE filter before the sample was injected into the HPLC. The concentrations of bismaleimide were measured by a Waters 2695 separations module equipped with a Luna C18 (Phenomenex, Part No. 00G-4041-E0) HPLC column and a Waters 2998 PDA detector, set at 320 nm. The temperature of the HPLC column was maintained at 50°C. The mobile phase was a gradient methanol/water (with 0.1 wt% formic acid) at a constant flow rate of 1.0 mL min^{-1} (0.1 wt% formic acid water linearly changed to methanol in 20 min, pure methanol for 7 min, and methanol was linearly changed to 0.1% formic acid water in 3 min). The concentrations of maleimide were measured by a Water 2695 separation module equipped with an Aminex HPX-87H (Bio-Rad) column and RI detector. The temperature of the HPLC column was maintained at 50°C, and the flow rate of the mobile phase (pH 2 water, acidified by sulfuric acid) was 0.6 mL min^{-1}.

GC-FID analysis of PHAH and FHAH. Partially-hydrogenated HAH (PHAH) and fully-hydrogenated HAH (FHAH) were quantified by gas chromatograph (Shinadzu GC-2010) equipped with a flame-ionization detector (GC-FID) and a Zebron ZB-50 column (Phenomenex, Part No. 7HG-G004-11). The hydrogenated HAH solutions (without dilution) were filtered with 0.2 µm PTFE membrane syringe filter before GC analysis. Analytical standards of PHAH and FHAH were synthesized and GC was calibrated with these analytical standards.

NMR analysis of biomass-derived monomers and polymers. ^1H nuclear magnetic resonance (NMR) and ^{13}C NMR spectrum were obtained by using Brucker Avance-500 spectrometer. Tetramethylsilane (TMS) (δ: 0 ppm) was used as a reference for chemical shifts in ^1H NMR spectrums and absolute reference was used for HSQC and ^{13}C NMR spectrum.

GPC analysis of polymers. Gel permeation chromatography (GPC) analysis was performed by using a Viscotek GPCmax/VE 2001 instrument fitted with PolyPore columns (2×300×7.5 mm) featuring 5 µm particle size from Polymer Laboratories. Liquid solution, containing the dissolved polymers in THF (<1mg mL^{-1}), was eluted with THF at a flow rate of 1 mL·min^{-1} at 40°C. The molecular weights of the dissolved polymers were characterized by UV (at 390 nm wavelength for HAH-MDI and HAH-SA, at 320 nm for other polyurethanes) detection using a Viscotek Model 302-050 Tetra Detector Array. Omnisec software (Viscotek, Inc.) was used for data processing such as positioning the baseline, setting limits, and applying the molecular weight calibration (polystyrene was used to calibrate GPC).

DSC analysis of polyurethanes. Differential scanning calorimetry (DSC) measurements (TA Instruments Q100 modulated differential scanning calorimeter, New Castle, DE) was used for investigating the phase transition of polyurethanes with a heating and cooling rate of 10°C min^{-1}. 5mg of polyurethanes were placed in the standard aluminum pan (TA instrument) and sealed by the standard aluminum lid (TA instrument) to prepare DSC samples. Empty standard aluminum pan and lid were sealed and used as a reference. The heating and cooling cycles were repeated 3 times between 30 to 250°C (300°C for HAH-MDI, 270°C for EG-MDI, 200°C for HAH-SA) under 50 mL min^{-1} of N_2 gas flow. 2 min of isotherm was allowed at the end of the heating and cooling process. DSC data were analyzed by TA Universal Analysis software. The specific heat capacity was calculated from the DSC result by using the equation: Specific heat capacity (C_p, J $°C^{-1}g^{-1}$) = Heat flow (W g^{-1}) * 60 (s min^{-1}) / Heating rate (10°C min^{-1})

TGA analysis of polyurethanes. TA Instruments Q500 Thermogravimetric Analyzer (TGA) was used for measuring the thermal stabilities of polyurethanes. 6 to 11 mg of polyurethanes were put in a 10 mm platinum sample pan with stirrup (Instrument Specialists Inc.) and placed in the furnace. Ramp rate was set to 20°C min^{-1} from 25°C (or 30°C) to 800°C (700°C for EG-MDI) under 50 mL min^{-1} of N_2 gas flow. TGA data were analyzed by TA Universal Analysis software.

DMA analysis of polyurethanes. TA RSA III Dynamic Mechanical Analysis (DMA) was used to measure the storage modulus (E') and loss modulus (E") of the molded polymers (Figure S14). Dynamic frequency sweep tests of the polymers were performed at a fixed force (0.03% of strain force for polyurethanes, 0.05% of strain force for polyester) from 0.01 to 20 Hz of strain rates. The temperature was maintained at 25°C during the measurements. tanδ = E"/E'.

ATR-FTIR analysis of molded polyurethanes. Attenuated total reflectance FTIR measurements (ATR-FTIR) were taken on a Bruker Vertex 70 equipped with a liquid nitrogen-cooled MCT detector. The ATR cell used was a MIRacle single reflection cell equipped with a diamond crystal (Pike Technologies). 20 mg of the molded polyurethanes (HAH-MDI, FHAH-MDI) were placed on ATR cell for the measurement. In a typical measurement, 128 scans were averaged with a 4 cm^{-1} resolution.

Preparation of Cu/γ-Al_2O_3 catalyst. The Cu/γ-Al_2O_3 catalyst was synthesized by ion exchange. Low soda gamma alumina (γ-Al_2O_3) was crushed and sieved to 80-150 mesh size and added to 150 mL of 18 MΩ Milli-Q water. The desired amount of tetraaminecopper (II) sulfate ($[Cu(NH_3)_4]SO_4{\cdot}_xH_2O$) was dissolved in a separate solution of 200 mL Milli-Q water and 0.5 M ammonium hydroxide solution.

The copper solution was added to the gamma alumina slurry and the pH was adjusted to 9 with 2 M sulfuric acid. This slurry was covered and stirred for 20 h, filtered by vacuum filtration, and washed with excess Milli-Q water until the rinse water was neutral. The resulting catalyst was dried overnight in vacuum oven (500-600 mbar) at 50℃. The dried catalyst was treated under flowing Ar gas (Airgas) at 300℃ (5℃/min heating rate, 30 min hold) and then at 400℃ (5℃/min, 3 h hold) under flowing H_2 gas (Airgas). Before cooling, the catalyst was held under Ar gas for 1 h at 400℃. The catalyst was then cooled in Ar gas and passivated for 30 min in flowing 1% O_2 in Ar gas (Airgas).

Production of HAH. 1.83 g of NaOH was dissolved in 15 g of Milli-Q water to prepare 3 M of NaOH solution to catalyze aldol-condensation and 2 mL of 37% HCl and 10 g of Milli-Q water were mixed to prepare 2 M of HCl solution to neutralize NaOH catalyst after aldol-condensation. 10.2 g of HMF, 3 mL of acetone, and 71.28 mL of Milli-Q water were mixed in 500 mL round bottom flask with magnetic stirring bar and placed in oil bath at 35℃ for 5 min. 6.67 mL of 3 M of NaOH solution was added to the HMF and acetone solution and the flask was capped with glass lid. After 1 h of aldol-condensation, ~7.74 mL of 2 M of HCl solution was added to the flask to terminate aldol-condensation by neutralization. A pH strip was used to measure the actual pH of the aldol-condensed solution. The aldol-condensed solution with the precipitated HAH was vacuum filtered by paper while rinsing with ~300 mL of Milli-Q water. The washed HAH was dried in a vacuum oven at 50℃, under 500-600 mbar for 2 days.

Partial hydrogenation of HAH. 100 mg of 3 wt% Cu/γ-Al_2O_3 catalyst was reduced at 300℃ for 5 h under 34 bar (at room temperature) of H_2 gas in a Parr reactor. HAH feed solution was prepared by dissolving 460 mg of HAH in 30 mL of IPA solvent. The HAH feed solution and a magnetic stirring bar were added into the 50 mL Parr reactor, containing the reduced Cu/γ-Al_2O_3 catalyst under Ar gas flow to avoid catalyst oxidation by air contact. The reactor was purged twice with 50 bar of Ar gas and three times with 30 bar of H_2 gas. The reactor was pressurized to 36 bar of H_2 gas at room temperature and was heated to 120℃ in 35 min (final pressure increased to 44 bar at 120℃). The reactor was kept at 120℃ for 12 h and cooled to room temperature by natural convection. The partially-hydrogenated product was separated from the solid catalyst by syringe filter. Solvent was evaporated by rotary evaporation (40℃, 30-100 mbar) and the product was characterized by ^{1}H and ^{13}C NMR and was quantified by GC-FID.

Full hydrogenation of HAH. 460 mg of HAH was dissolved in 30 mL of IPA solvent. 60 mg of 5 wt% Ru/C catalyst and the HAH solution were added into a 50 mL Parr reactor with a magnetic stirring bar. The reactor was purged twice with 50 bar of Ar gas and three times with 30 bar of H_2 gas. The reactor was pressurized to 30 bar of H_2 gas at room temperature and was heated to 180℃ in 1 h (final pressure increased to 55 bar at 180℃). The reactor was kept at 180℃ for 1 h and cooled to room temperature by natural convection. The fully-hydrogenated product was separated from the solid catalyst by a syringe filter. Solvent was evaporated by rotary evaporation (40℃, 30-100 mbar) and the product was characterized by ^{1}H and ^{13}C NMR and was quantified by GC-FID.

Diels-Alder reaction of maleimides and PHAH. 0.21 g of partially-hydrogenated HAH (PHAH, 0.74 mmol) and 0.21 g of maleimide (2.19 mmol) were dissolved in 4 mL of THF solvent to prepare a feed solution. A magnetic stirring bar was put into the feed solution and the solution was placed in oil bath at 50℃ for 93 h. 0.045 g (50μL) of solutions were diluted in 0.09 g (450μL) of Milli-Q water to prepare the HPLC samples. 0.11 g of PHAH-MDI polyurethane (0.15 mmol of PHAH unit) and 0.016 g of bismaleimide (0.04 mmol) were mixed in 2 mL of THF solvent with a magnetic stirring bar and placed in an oil bath at 50℃ for 69 h. 0.20 g of HAH-PHAH-MDI polyurethane (0.31 mmol of PHAH unit, 0.09 mmol of HAH unit) and 0.055 g of bismaleimide (0.15 mmol) were mixed in 4 mL of THF solvent with a magnetic stirring bar and placed in an oil bath at 50℃ for 70 h. The polyurethanes were swollen by THF solvent. 0.088 g (100μL) of solutions were diluted in 0.31 g (400μL) of acetone for HPLC analysis of bismaleimide concentration. After the Diels-Alder reaction, THF solvent was evaporated by rotary evaporation (40℃, 30-200 mbar) and the solid sample was washed by ~30 g of Milli-Q water. The washed polyurethanes were dried in a vacuum oven at 50℃, under 500-600 mbar for 1 day.

Synthesis of polyurethanes in a round bottom flask. Controlled amounts of polyols (HAH, PHAH, FHAH, ethylene glycol) were dissolved in DMSO solvent to prepare 2 M (2 mmol diols in 1 mL) of polyol feed solution. Controlled amounts of MDI were dissolved in MIBK solvent to prepare 2 M (2 mmol MDI in 1 mL) of MDI feed solution. The equivalent volume of the polyol solution and the MDI solution was used for synthesis of polyurethanes. Before mixing the monomer feed solutions, both polyol and MDI solutions were preheated at 115℃ for 12 min to remove the moisture in the solutions. The preheated MDI solution was added dropwise to the preheated polyol solution in a round bottom flask with a magnetic stirring bar, and the round bottom flask was capped by a glass lid during the reaction. DMSO/MIBK (1/1, v/v) co-solvent with half the volume of the mixed feed solution was prepared as an additional co-solvent and was added to the polyurethane solutions to reduce the viscosity when the magnetic stirring bar was stopped by high viscosity. Polyurethanes were synthesized within a few minutes (2-5 min), at which point the magnetic stirring bar was stopped by high viscosity or by the solvent-swollen polyurethanes. The reaction was terminated by pouring the polyurethane solutions into 200 mL of Milli-Q water at room temperature. The polyurethanes were rinsed by 200 mL of Milli-Q water 3 times and dried in vacuum oven at 50℃, under 500-600 mbar for 1 day.

Synthesis of molded polyurethanes and polyurethane coatings. 0.508 g of MDI (2 mmol) was dissolved in 0.653 g of MIBK (0.81 mL), and 0.550 g of HAH (2 mmol) was dissolved in 0.892 g of DMSO (0.81 mL). Both feed solutions were preheated at 115℃ for 12 min to remove moisture in the solutions. The preheated HAH and MDI solutions were mixed on a glass dish by a metal spatula at room temperature. Then, the mixed monomer solution was placed in a circular (25 mm diameter) aluminum mold and cured on the hot plate at 95℃ for 10 min. The mold was placed in a vacuum oven at 50℃, under 500-600 mbar (house vacuum) for 20 h to evaporate DMSO and MIBK solvents. 0.619 g of MDI (2.5 mmol) was dissolved in 0.790 g of MIBK (0.99 mL), and 0.710 g of FHAH (2.5 mmol) was dissolved in 1.091 g of DMSO (0.99 mL). Both feed solutions were

preheated at 115℃ for 12 min to remove moisture in the solutions. The preheated FHAH and MDI solutions were mixed on a glass dish by a metal spatula at room temperature. Then, the mixed monomer solution was placed in a circular (25 mm diameter) aluminum mold and cured on the hot plate at 80℃ for 10 min. The mold was placed in a vacuum oven at 50℃, under 500-600 mbar (house vacuum) for 23 h to evaporate DMSO and MIBK solvents. The glass dish with the thin layer of the mixed monomer solution was cured at 80-95℃ for 10 min to produce the hydrophobic coating (Figure S13).

Synthesis of molded polyester. 0.69 g (2.5 mmol) of HAH and 0.30 g (2.5 mmol) of succinic acid were dissolved in 1 mL of DMSO at room temperature to prepare a monomer feed solution. 0.03 g (0.1 mmol) of dibutyltin oxide was dissolved in the feed solution at 130℃ for 5 min to form a homogeneous solution. The homogeneous solution was placed into a rectangular Al mold (L:42 x W:10 x H:5 mm) and reacted on the hot plat, set at 180℃ for 70 min. Then, the temperature of the hot plate decreased to 140℃ and kept for 17 h for DMSO evaporation and curing the polyester.

Tracking esterification during polyester synthesis. 0.69 g of HAH, 0.30 g of succinic acid, and 0.03 g of dibutyltin oxide were mixed with 1 mL of DMSO-d_6 solvent in glass vial and placed in oil bath at 130℃ with stirring bar (300 rpm). The glass vial was not capped by a lid to allow the evaporation of water by-product. 0.05 g of polymeric solution was diluted in 0.67 g of DMSO-d_6 at different reaction times (60, 300, 470, 870 min) for NMR analysis. After 470 min reaction, 3 g of DMSO-d_6 was added to re-dissolve the cured polyester.

Conclusions

We synthesized HAH from a biomass-derived platform chemical (HMF) by aldol-condensation, and the HAH monomer was selectively upgraded to different functional monomers by hydrogenation over Cu or Ru catalysts in high yield (≥91 mol%). Selective hydrogenation of HAH enables changes in chemical functionalities of each monomer. As a result, biomass-derived monomers, such as HAH, PHAH, and FHAH, were demonstrated to become functional monomers for production of various polymers with UV absorption properties, binding sites for Diels-Alder reactions, and crosslinking ability. The high UV absorbance, sp^2 carbon-based rigid frame, thermal, and mechanical properties of HAH-derived polymers indicate that these materials can be used in UV-block coatings, thermal insulators, and packaging applications. The Diels-Alder reaction of PHAH units provides tunable thermal stability of polyurethanes and also could be used to deliver maleimide-based antimicrobial chemicals[36,37] or to synthesize self-healing functional polyurethanes[38]. FHAH is a flexible symmetric triol and can be used to produce an energy-dissipating rubber for packaging or coating applications. It could be a substitute for glycerol that serves as a crosslinking agent to synthesize branched polymers[12]. HAH, PHAH and FHAH can be blended with each other or with petroleum-based diols (such as ethylene glycol) to further tune the properties and produce sustainable, economically viable, performance-advantaged polymers. For commercial production of HAH-derived polymers, future work may be required to replace high boiling point solvents, such as DMSO and MIBK, with other solvents that can be more economically removed from the polymers and recycled at the industrial scale.

Author Contributions

Hochan Chang contributed conceptualization, data curation, formal analysis, investigation, methodology, resources, validation, visualization, and writing; James A. Dumesic and George W. Huber contributed conceptualization, project administration, funding acquisition, supervision, and writing; Elise B. Gilcher contributed data curation and writing.

Conflicts of interest

Hochan Chang, George W. Huber, and James A. Dumesic have submitted a patent application related to this work filed by the Wisconsin Alumni Research Foundation (Application no. 17/186,744). Elise B. Gilcher declare that they have no competing interests.

Acknowledgements

We thank Shao-Chun Wang for help in ATR-FTIR measurement and analysis. the NMR facilities that are funded by: Thermo Q ExactiveTM Plus by NIH 1S10 OD020022-1; Bruker Quazar APEX2 and Bruker Avance-500 by a generous gift from Paul J. and Margaret M. Bender; Bruker Avance-600 by NIH S10 OK012245; Bruker Avance-400 by NSF CHE-414 1048642 and the University of Wisconsin-Madison; **Funding:** This material is based upon work supported in part by U.S. Department of Energy under Award Number DE-EE0008353; this material is also based upon work supported by the U.S. Department of Energy, Office of Science, Office of Basic Energy Sciences, Chemical Sciences, Geosciences, and Biosciences Division, under Contract DE-SC0014058.

Notes and references

1 H. Chang, I. Bajaj, A. H. Motagamwala, A. Somasundaram, G. W. Huber, C. T. Maravelias and J. A. Dumesic, *Green Chem.*, , DOI:10.1039/d1gc00311a.
2 D. M. Alonso, S. G. Wettstein and J. A. Dumesic, *Chem. Soc. Rev.*, 2012, **41**, 8075–8098.
3 T. Wang, M. W. Nolte and B. H. Shanks, *Green Chem.*, 2014, 16, 548–572.
4 H. Chang, I. Bajaj, G. W. Huber, C. T. Maravelias and J. A. Dumesic, *Green Chem.*, 2020, **22**, 5285–5295.
5 US4243493A, 1981.
6 M. Wang, H. Lee and J. Molburg, *Int. J. Life Cycle Assess.*, 2004, **9**, 34–44.
7 G. A. Buchner, N. Wulfes and R. Schomäcker, *J. CO2 Util.*, 2020, **36**, 153–168.
8 Chemical profile: US ethylene glycol | ICIS, https://www.icis.com/explore/resources/news/2013/03/08/9647891/chemical-profile-us-ethylene-glycol/, (accessed 10 December 2020).
9 J. O. Akindoyo, M. D. H. Beg, S. Ghazali, M. R. Islam, N.

Jeyaratnam and A. R. Yuvaraj, *RSC Adv.*, 2016, 6, 114453–114482.

10 X. Yu, B. P. Grady, R. S. Reiner and S. L. Cooper, *J. Appl. Polym. Sci.*, 1993, **49**, 1943–1955.

11 R. W. Thring, M. N. Vanderlaan and S. L. Griffin, *Biomass and Bioenergy*, 1997, **13**, 125–132.

12 T. Zhang, B. A. Howell, A. Dumitrascu, S. J. Martin and P. B. Smith, *Polymer*, 2014, **55**, 5065–5072.

13 US4340526A, 1982.

14 A. R. Webb, J. Yang and G. A. Ameer, *Expert Opin. Biol. Ther.*, 2004, 4, 801–812.

15 A. M. Diciccio and G. W. Coates, *J. Am. Chem. Soc.*, 2011, **133**, 10724–10727.

16 N. A. Peppas and J. Klier, *J. Control. Release*, 1991, **16**, 203–214.

17 G. X. De Hoe, M. T. Zumstein, B. J. Tiegs, J. P. Brutman, K. McNeill, M. Sander, G. W. Coates and M. A. Hillmyer, *J. Am. Chem. Soc.*, 2018, **140**, 963–973.

18 P. Alagi, Y. J. Choi and S. C. Hong, *Eur. Polym. J.*, 2016, **78**, 46–60.

19 R. O. Rajesh, T. K. Godan, R. Sindhu, A. Pandey and P. Binod, *Bioengineered*, 2020, **11**, 19–38.

20 L. Sun, J. Wang, S. Mahmud, Y. Jiang, J. Zhu and X. Liu, *Eur. Polym. J.*, 2019, **118**, 642–650.

21 N. Warlin, M. N. Garcia Gonzalez, S. Mankar, N. G. Valsange, M. Sayed, S. H. Pyo, N. Rehnberg, S. Lundmark, R. Hatti-Kaul, P. Jannasch and B. Zhang, *Green Chem.*, 2019, **21**, 6667–6684.

22 S. K. R. Patil and C. R. F. Lund, *Energy and Fuels*, 2011, **25**, 4745–4755.

23 Y.-Y. Wang, C. E. Wyman, C. M. Cai and A. J. Ragauskas, *ACS Appl. Polym. Mater.*, 2019, **1**, 1672–1679.

24 Y. Li and S. Sarkanen, *Macromolecules*, 2002, **35**, 9707–9715.

25 H. Chang, A. H. Motagamwala, G. W. Huber and J. A. Dumesic, *Green Chem.*, 2019, **21**, 5532–5540.

26 J. S. Luterbacher, J. M. Rand, D. M. Alonso, J. Han, J. T. Youngquist, C. T. Maravelias, B. F. Pfleger and J. A. Dumesic, *Science*, 2014, **343**, 277–280.

27 K. Xiong, W. Wan and J. G. Chen, *Surf. Sci.*, 2016, **652**, 91–97.

28 A. V. Mironenko and D. G. Vlachos, *J. Am. Chem. Soc.*, 2016, **138**, 8104–8113.

29 Y. Fang, X. Du, Y. Jiang, Z. Du, P. Pan, X. Cheng and H. Wang, *ACS Sustain. Chem. Eng.*, 2018, **6**, 14490–14500.

30 H. Chang, G. W. Huber and J. A. Dumesic, *ChemSusChem*, 2020, **13**, 5213–5219.

31 A. Demharter, *Cryogenics*, 1998, **38**, 113–117.

32 C. Kim and J. R. Youn, *Polym. - Plast. Technol. Eng.*, 2000, **39**, 163–185.

33 I. Meynial-Salles, S. Dorotyn and P. Soucaille, *Biotechnol. Bioeng.*, 2008, **99**, 129–135.

34 H. Choudhary, S. Nishimura and K. Ebitani, *Appl. Catal. A Gen.*, 2013, **458**, 55–62.

35 D. R. Vardon, M. A. Franden, C. W. Johnson, E. M. Karp, M. T. Guarnieri, J. G. Linger, M. J. Salm, T. J. Strathmann and G. T. Beckham, *Energy Environ. Sci.*, 2015, **8**, 617–628.

36 K. Takatori, T. Hasegawa, S. Nakano, J. Kitamura and N. Kato, *Microbiol. Immunol.*, 1985, **29**, 1237–1241.

37 A. A. Panov, S. N. Lavrenov, A. Y. Simonov, E. P. Mirchink, E. B. Isakova and A. S. Trenin, *J. Antibiot. (Tokyo).*, 2019, **72**, 122–124.

38 Y. Fang, X. Du, Y. Jiang, Z. Du, P. Pan, X. Cheng and H. Wang, *ACS Sustain. Chem. Eng.*, 2018, **6**, 14490–14500.